Investigation of Facilitated Ion−Transfer Reactions at High Driving Force by Scanning Electrochemical Microscopy

ARTICLE *in* THE JOURNAL OF PHYSICAL CHEMISTRY B · FEBRUARY 2004

Impact Factor: 3.3 · DOI: 10.1021/jp037498m

Anal. Chem. **2003,** *75,* 6593−6601

Studies of Electron-Transfer and Charge-Transfer Coupling Processes at a Liquid/Liquid Interface by Double-Barrel Micropipet Technique

Yong Chen,[†] Zhao Gao,[†] Fei Li,[†] Liaohai Ge,[†] Meiqin Zhang,[†] Dongping Zhan,[‡] and Yuanhua Shao*,[†,‡]

State Key Laboratory of Electroanalytical Chemistry, Changchun Institute of Applied Chemistry, Chinese Academy of Sciences, Changchun 130022, China, and College of Chemistry and Molecular Engineering, Peking University, Beijing 100871, China

Investigation of a heterogeneous electron-transfer (ET) reaction at the water/1,2-dichloroethane interface employing a double-barrel micropipet technique is reported. The chosen system was the reaction between $Fe(CN)_6^{3-}$ in the aqueous phase (W) and ferrocene in 1,2-dichloroethane (DCE). According to the generation and the collection currents as well as collection efficiency, the ET−ion-transfer (IT) coupling process at such an interface and competing reactions with the organic supporting electrolyte in the organic phase can be studied. In addition, this technique has been found to be an efficient method to distinguish and measure the charge-transfer coupling reaction between two ions (IT−IT) processes occurring simultaneously at a liquid/liquid interface. On this basis, the formal Gibbs energies of transfer of some ions across the W/DCE interface, such as NO_3^-, NO_2^-, Cl^-, COO^-, TBA^+, $TPAs^+$, Cs^+, Rb^+, K^+, Na^+, and Li^+, for which their direct transfers are usually difficult to obtain because of the IT−IT coupling processes, were quantitatively evaluated.

Micropipet voltammetry was first introduced by Taylor and Girault employing a micropipet to construct a micro-liquid/liquid (L/L) interface in 1986.[1] This method has been applied to investigate the mechanism and thermodynamics of various electron-transfer (ET) and ion-transfer (IT) processes at L/L interfaces,[2−13] because it can effectively overcome the problems arising from the charge current and resistive effects, which often interfere with electrochemical measurements at the conventional (mm-sized) L/L interface.[14] However, micropipet techniques have not been widely used for studying the charge-transfer coupling (CTC) processes at a L/L interface. CTC processes are usually involved simultaneously as ET and IT or IT−IT reactions at a L/L interface; hence, they interfere with each other (see Figure 1). CTC processes are common phenomena, which usually take place in complicated systems and play an important role in many chemical and biological systems, such as phase-transfer catalysis, and processes involved at biological membranes.[15]

Some generation/collection (G/C) techniques have been recently introduced to the electrochemistry at L/L interfaces and been employed successfully for studying the mechanism and kinetics of some coupling charge-transfer reactions at such interfaces and probing charge/mass transport in various media, such as scanning electrochemical microscopy[16] and microelectrochemical measurement at expanding droplets.[17] In addition, a novel G/C technique for studying ionic reactions was first introduced by Shao et al. and applied successfully to probe the simple IT and the facilitated ion transfer (FIT) across the aqueous phase (W)/1,2-dichloroethane (DCE) interface based on dual pipets, namely, double-barrel micropipets.[18] Compared with the

* To whom correspondence should be addressed. Fax: +86-10-62751708. E-mail: yhshao@chem.pku.edu.cn.

[†] Chinese Academy of Sciences.

[‡] Peking University.

(1) Taylor, G.; Girault, H. H. *J. Electroanal. Chem.* **1986**, *208*, 179−183.
(2) Campbell, J. A.; Stewart, A. A.; Girault, H. H. *J. Chem. Soc., Faraday Trans.* **1989**, *85*, 843−853.
(3) Stewart, A. A.; Shao, Y.; Pereira, C. M.; Girault, H. H. *J. Electroanal. Chem.* **1991**, *305*, 135−139.
(4) Stewart, A. A.; Taylor, G.; Girault, H. H. *J. Electroanal. Chem.* **1990**, *296*, 491−515.
(5) Kakutani, T.; Nishiwakim, Y.; Osakai, T.; Senda, M. *Bull. Chem. Soc. Jpn.* **1986**, *59*, 781−788.
(6) Shao, Y.; Girault, H. H. *J. Electroanal. Chem.* **1992**, *334*, 203−211.
(7) Beattie, P. D.; Delay, A.; Girault, H. H. *J. Electroanal. Chem.* **1995**, *380*, 167−175.
(8) Kontturi, A.; Kontturi, K.; Murtomäki, L.; Quinn, B.; Cunnane, V. J. *J. Electroanal. Chem.* **1997**, *424*, 69−74.
(9) Shao, Y.; Mirkin, M. V. *Anal. Chem.* **1998**, *70*, 3155−3161.
(10) Horrocks, B. R.; Mirkin, M. V. *Anal. Chem.* **1998**, *70*, 4653−4660.
(11) Biao, L.; Mirkin, M. V. *Electroanalysis* **2000**, *12*, 1443−1446.
(12) Yuan, Y.; Shao, Y. *J. Phys. Chem. B.* **2002**, *106*, 7809−7814.
(13) Su, B.; Zhang, S.; Yuan, Y.; Guo, J.; Gan, L.; Shao, Y. *Anal. Chem.* **2002**, *74*, 373−378.
(14) Girault, H. H. In *Modern Aspects of Electrochemistry*; Bockris, J. O., Conway, B. E., White, R. E., Eds.; Plenum Press: New York, 1993; Vol. 13, p 31.
(15) (a) Nicholls, D. G.; Ferguson, S. G. *Bioenergetics 2*; Academic Press: London, 1992. (b) Cunnane, V. J.; Schiffrin, D. J.; Beltran, C.; Geblewicz, G.; Solomon, T. *J. Electroanal. Chem.* **1988**, *247*, 203−214. (c) Maeda, K.; Kihara, S.; Suzuki, M.; Matsui, M. *J. Electroanal. Chem.* **1991**, *303*, 171−184. (d) Kakiuchi, K. *Electrochim. Acta* **1995**, *40*, 2999−3003.
(16) (a) Wei, C.; Bard, A. J.; Mirkin, M. V. *J. Phys. Chem.* **1995**, *99*, 16033−16042. (b) Selzer, Y.; Turyan, I.; Mandler, D. *J. Phys. Chem. B.* **1999**, *103*, 1509−1517. (c) Selzer, Y.; Mandler, D. *J. Phys. Chem. B.* **2000**, *104*, 4903−4910.
(17) Zhang, J.; Slevin, C. J.; Unwin, P. R. *Chem. Commun.* **1999**, 1501−1502.
(18) Shao, Y. H.; Liu, B.; Mirkin, M. V. *J. Am. Chem. Soc.* **1998**, *120*, 12700−12701.

10.1021/ac034674e CCC: $25.00
Published on Web 10/29/2003

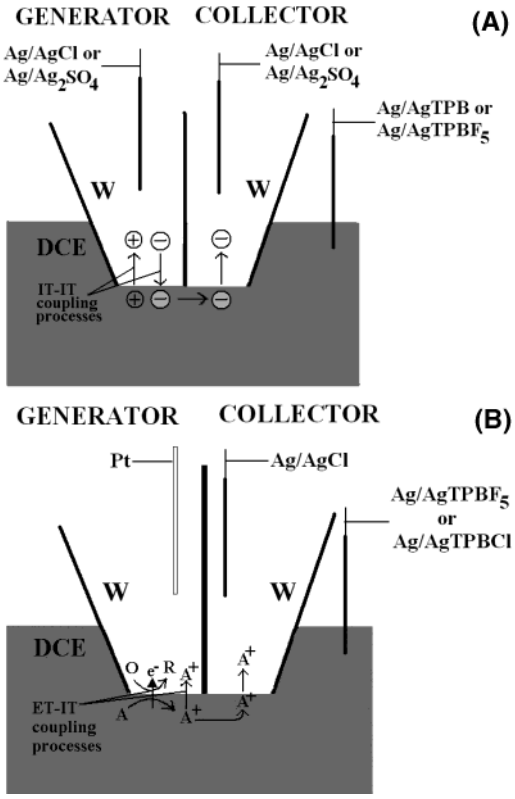

Figure 1. Schematic diagrams of charge-transfer reaction at the liquid/liquid interface. (A) Cation−anion coupling transfer processes. (B) Electron-transfer coupling with ion-transfer processes.

hydrodynamically controlled and geometrically well-defined classical G/C setup, such as the rotating ring−disk electrode, there is a somewhat limited level of available mathematical treatment for the processes at a tip of a double-barrel micropipet because its geometry is more complicated and the well-described transport theory is absent. However, this G/C technique is useful for studying those ionic reactions involving no redox species, because in this technique, the generator and collector are different from that of a classical G/C technique: two L/L interfaces formed between the aqueous solution in each pipet and the outer organic solution can serve as the generator and the collector, so that charge (electron and ion)-transfer behaviors across two immiscible liquids, rather than redox processes, can be studied under applied potentials. Moreover, it was found that the double-barrel micropipet technique could study not only the homogeneous reaction in the organic phase but also the IT−IT coupling process across a L/L interface.[19] This technique can be considered as a promising method for studying other type charge-transfer reactions occurring at a L/L interface, such as ET reactions, ET−IT and IT−IT coupling processes, which are illustrated in Figure 1.

ET reactions at various L/L interfaces have not been investigated by this technique so far; therefore, our present work is mainly aimed to apply this technique to probe ET and the processes of coupling ET−IT and IT−IT. Here, we investigated the redox reaction between ferrocene (Fc) in the organic phase (DCE) and $Fe(CN)_6^{3-}$ in the aqueous phase (W). Although there have been a large number of reports on this system, there are still some conflicting views mainly about its various side reactions, including a possible homogeneous ET reaction and competing reaction with the organic supporting electrolyte, as well as the ET−IT coupling process.[20] This system also provides a good example of an ET−IT coupling reaction at a L/L interface. To understand it more fully, the double-barrel micropipet technique has been employed to explore this system, which involves multistep mechanisms of coupling processes and homogeneous reactions. Additionally, the IT−IT coupling processes at the W/DCE interface, especially appearing at the positive and negative ends of the potential window, have been also studied in detail by this technique.

EXPERIMENTAL SECTION

Chemicals. $NaNO_2$, $NaClO_4$, $LiNO_3$, LiCl, NaCl, KCl, RbCl, CsCl, Li_2SO_4, $K_4Fe(CN)_6$, $K_3Fe(CN)_6$, trimethylchlorosilane (99%), sodium tetraphenylborate (NaTPB, 99%), and 1,2-dichloroethane (99.8%) were obtained from Beijing Chemical Co. Ferrocene (98%, Acros), bis(triphenylphosphoranylidene)ammonium chloride (Fluka), lithium tetrakis(pentafluorophenyl)borate (Fluka), tetraphenylarsonium chloride (TPAsCl, 97%, Aldrich), potassium tetrakis(4-chlorophenyl)borate (98%, Fluka), and tetrabutylammonium chloride (TBACl, 99%, Fluka) were used as received. Bis(triphenylphosphoranylidene)ammonium tetraphenylborate, bis(triphenylphosphoranylidene)ammonium tetrakis(pentafluorophenyl)borate, tetraphenylarsonium tetrakis(pentafluorophenyl)-borate ($TPAsTPBF_5$), tetrabutylammonium tetrakis(pentafluorophenyl)borate ($TBATPBF_5$), and tetrabutylammonium tetrakis(4-chlorophenyl)borate (TBATPBCl) were prepared as described previously[21,22] and served as the supporting electrolytes for the organic phase. All reagents were of analytical grade. The aqueous and organic phases were prepared with deionized water (Milli-Q, Millipore Corp.) and DCE, respectively. DCE was washed several times with deionized water before use. Special precautions were taken for dealing with DCE and other hazardous chemicals.

Fabrication and Silanization of Double-Barrel Micropipets. Double-barrel micropipets were made from borosilicate glass capillaries (o.d., 1.5 mm, length, 10 cm) by a laser-based pipet puller model P-2000 (Sutter Instrument Co.). The appropriate pulling programs were developed to fabricate short-shank (patch-type) pipets in order to minimize the *iR* drop inside the narrow shaft. To prevent the formation of an aqueous film between two pipets and mixing of the filling solutions, the outer surface of the pipet was silanized, which was done by dipping the pipet tip into trimethylchlorosilane for 1−2 min, while passing a fast flow of argon through the pipet from the back and then keeping the flow of argon after drawing the pipet out of the trimethyl-

(19) Liu, B.; Shao, Y. H.; Mirkin, M. V. *Anal. Chem.* **2000**, *72*, 510−519.

(20) (a) Samec, Z.; Mareček, V.; Weber, J. *J. Electroanal. Chem.* **1979**, *96*, 245−247. (b) Hanzlík, J.; Samec, Z.; Hovorka, J. *J. Electroanal. Chem.* **1987**, *216*, 303−308. (c) Cunnane, V. J.; Geblewicz, G.; Schiffrin, D. J. *Electrochim. Acta* **1995**, *40*, 3005−3014. (d) Quinn, B.; Lahtinen, R.; Murtomäki, L.; Kontturi, K. *Electrochim. Acta* **1998**, *44*, 47−57. (e) Quinn, B.; Kontturi, K. *J. Electroanal. Chem.* **2000**, *483*, 124−134. (f) Zhang, Z.; Yuan, Y.; Sun, P.; Su, B.; Guo, J.; Shao, Y.; Girault, H. H. *J. Phys. Chem. B* **2002**, *106*, 6713−6717.

(21) Fermin, D. J.; Duong, H. D.; Ding, Z.; Brevet, P.; Girault, H. H. *Phys. Chem. Chem. Phys.* **1999**, *1*, 1461−1467.

(22) Kontturi, A. K.; Murtomaki, L.; Schiffrin, D. J. *J. Chem. Soc., Faraday Trans.* **1994**, *90*, 2037−2041.

chlorosilane solution for 1 min to avoid silanization of the inner wall of the pipet. All prepared micropipets were inspected using an Olympus BX-60 microscope (×100−×500) prior to experiments. The scanning electron microscopy (SEM) image of the double-barrel micropipet was obtained with a JXA-840 SEM (JEOL).

Electrochemical Cells and Measurements. Electrochemical measurements were carried out in a three-electrode mode as described previously.[18,19] The pipets were filled with aqueous solution from the back using a small (10 μL) syringe. A 0.125-mm silver wire coated with either AgCl or Ag_2SO_4 was inserted into each pipet from the back and employed as the aqueous reference electrode, but in the ET experiments, a 0.125-mm platinum wire was used as the pseudoreference electrode and inserted into the generator pipet. In addition, a 0.2-mm silver wire coated with AgTPB, AgTPBCl, or $AgTPBF_5$ was inserted in the outer DCE solution and served as the organic reference electrode. Cyclic voltammetry was performed using a bipotentiastat (CHI 900, CH Instruments) to control the potentials of two pipets serving as working electrodes with respect to the organic reference electrode. The cells used in the experiments are shown below. The double lines here indicate the W/DCE interfaces,

where AB in cell 2 refers to the organic supporting electrolyte. x and Y in cells 3 and 4 are the respective concentration and species we are going to study. In addition, the positive current refers to the transfer of positive charge from the aqueous to the organic phase or negative charge from the organic to the aqueous phase, and the negative current refers to the transfer of positive charge from the organic to the aqueous phase or negative charge from the aqueous to the organic phase. All experiments were carried out at room temperature (25 ± 2 °C).

RESULTS AND DISCUSSION

In this G/C technique employing the double-barrel micropipet, two micro-L/L interfaces were created by linking the outer organic solution with two unattached aqueous solutions filled separately in the channels of the pipet, the orifice of which consisted of two micrometer-sized elliptic pipets separated by a very thin band of glass (≤1 μm) (see the SEM image of a double-barrel micropipet shown in Figure 2). For an IT G/C experiment including simple IT or FIT, the IT reactions occur at one of the pipets (generator) by cyclically scanning it with respect to the external reference electrode; then a significant fraction of product can be collected at the other pipet (collector) by holding it at a corresponding

Cell 1

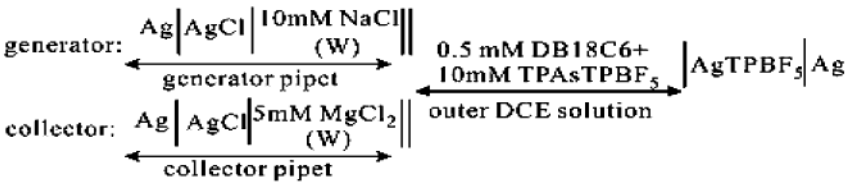

Cell 2

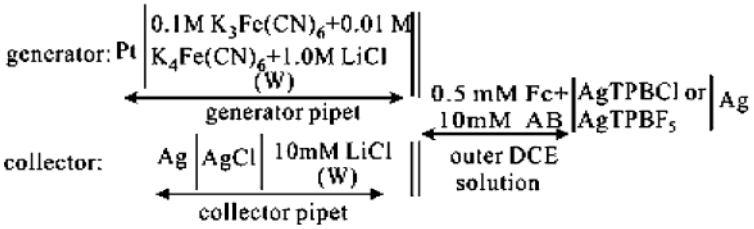

Cell 3

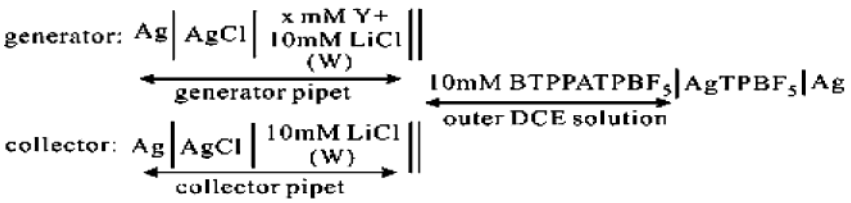

Cell 4

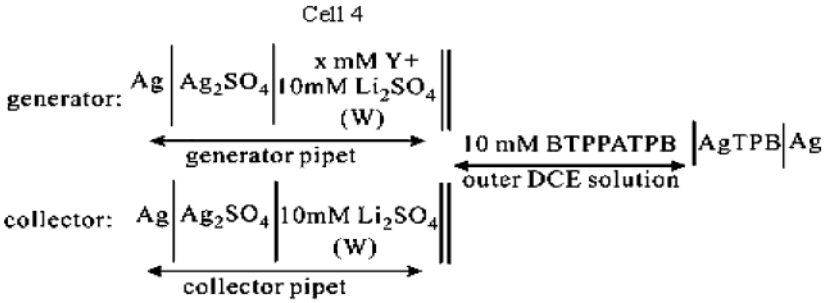

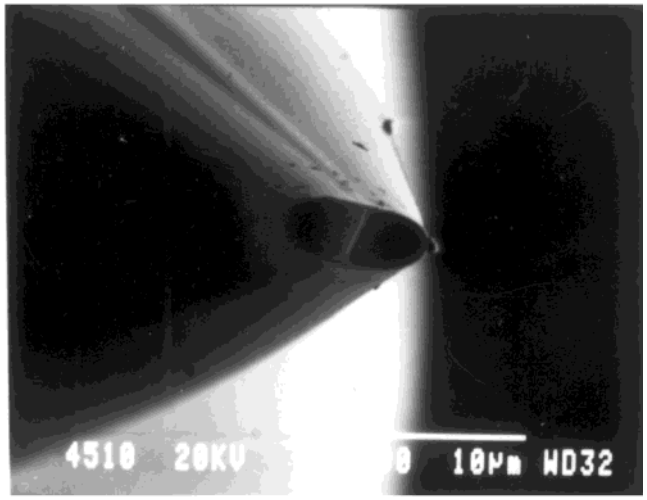

Figure 2. SEM image of the orifice of a double-barrel micropipet. Both of their orifices were 2.5 μm in radius.

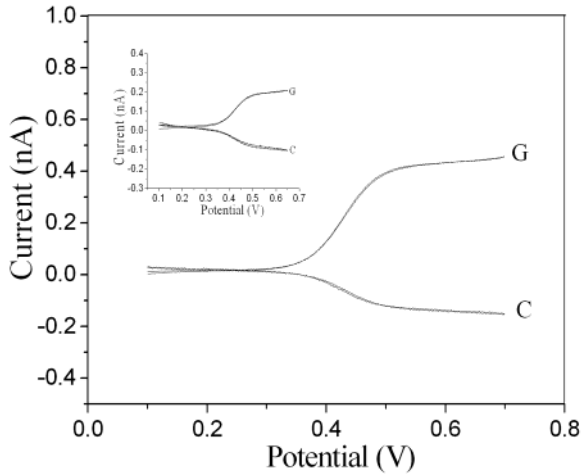

Figure 3. Generation and collection (G/C) voltmmograms of facilitated sodium transfer by DB18C6 across the W/DCE interface using cell 1. Both orifices of the double-barrel micropipet were 5-μm radius. The collector potential (E_c) was held at 0.1 V vs Ag/AgTPBF$_5$. The scan rate was 10 mV/s. The inset showed such FIT G/C voltammograms with higher collection efficiency (η_{max} = 45%). The radii of generator and collector pipets are $r_g = r_c = 2$ μm.

potential. It has been found that both the generation and the collection voltammograms (G/C) of potassium ion transfer facilitated by DB18C6 across the W/DCE interface were well-defined steady-state sigamoidal waves due to the spherical or hemispherical diffusion of ionophore in the outer solution to the orifice of generator,[18] which can also be demonstrated by the G/C voltammograms of sodium FIT reaction across W/DCE interface (see the Figure 3). According to the steady-state currents of generator (i_g) and collector (i_c), the maximum of collection efficiency (i.e., the ratio of two currents, $\eta = i_c/i_g$) is calculated to be 35%, and its higher value (45%) can be obtained by employing anothor pipet (see the inset in Figure 3), which is close to that reported previously.[18,19] It is apparent that collection efficiency depends on the geometry of a double-barrel micropipet. Similar procedures were adapted in the following experiments.

ET and ET−IT Coupling Processes. Figure 4A showed an example for the G/C voltammograms of a heterogeneous ET reaction between Fc in the DCE phase and $Fe(CN)_6^{3-}$ in the

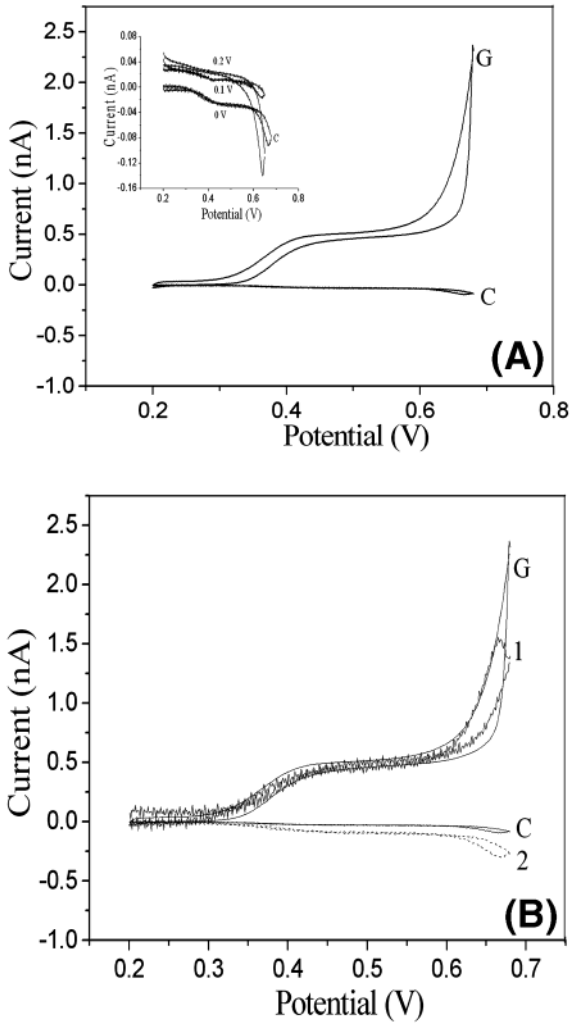

Figure 4. (A) G/C voltammograms of ET with TBATPBF$_5$ as the organic supporting electrolytes. E_c was 0 V vs Ag/AgTPBF$_5$. The inset was the collection voltammograms obtained at different collecting potentials. (B) Separation of ET−IT coupling processes. Dashed line 1 was the generation voltammogram reconstructed from the i_c vs E_g data as demonstrated in the text. The coupling IT process at the generator (dashed line 2) was obtained using eq 2. Both orifices of the double-barrel micropipet were 5 μm in radius. Scan rate was 10 mV/s.

aqueous phase employing cell 2, where TBATPBF$_5$ was used as the organic supporting electrolyte. As expected, a heterogeneous ET process occurred at the generator, and then a fraction of ET product ferricenium (Fc^+) could reach and transfer back into the collector at a collector potential (E_c), which could be expressed as follows:

$$Fc(DCE) + Fe(CN)_6^{3-}(W) \rightleftharpoons Fc^+(DCE) + Fe(CN)_6^{4-}(W) \quad \text{(ET at generator)}$$

$$Fc^+(DCE) \rightarrow Fc^+(W) \quad \text{(IT at collector)}$$

Figure 4A showed a typical steady-state wave (curve G) for this ET process occurring at a generator pipet, and the generation current is limited by a spherical or hemispherical diffusion of Fc in the DCE phase as long as its concentration is much lower than

the reactant concentration inside the generator pipet. Meanwhile, at $E_c = 0$ V, a steady-state collection voltammogram (curve C in the inset of Figure 4A) was also obtained, which should correspond to the transfer of Fc^+ from the organic phase into the aqueous solution in the collector.

We also found that the collection current, similar to that of FIT, strongly depended upon the collecting potential, which led to the collection efficiency being increased from 0 to the maximum with decrease of the collector potential from 0.2 to 0 V (see the insets in Figure 4A). The supporting electrolytes in both phases will severely affect the collection voltammograms if the potential is applied more negatively than 0 V. However, the maximum of collection efficiency ($\eta_{max} = 6\%$) is much lower than the value (35%) obtained in the FIT G/C experiments using a pipet with similar geometry (see Figure 3). Based on these facts and previous reports,[20] such low collection efficiency for the ET can be attributed to the homogeneous ET reaction or ET−IT coupling at the generator resulting in the flow of some reactant Fc or ET product Fc^+ from the DCE phase to the aqueous solution in the generator or to the intrinsic slowness of Fc^+ from the DCE phase to the aqueous solution in the collector. Considering the salting-out effect of the highly concentrated aqueous electrolyte used in the generator (1.0 M) and the steady-state waves of the generation voltammogram obtained in the experiments, it is almost impossible for a homogeneous ET reaction in the aqueous solution of generator, but it is possible for an ET−IT coupling reaction to occur at the generator because of Gibbs energy coupling of IT-ET or equilibrium ET. According to $i_g = i_c/\eta_{max}$, it should be possible to reconstruct the generation voltammogram from i_c versus E_g dependence. An example of such a reconstruction is shown in Figure 4B, where the generation voltammogram (curve 1) was caculated from the collection voltammogram (curve C) using the above eqation with $\eta_{max} = 6\%$. A perfect agreement between calculated and measured i_g values (curves 1 and G) proves the validity of the reconstruction, which also confirmed that the collector voltammogram indeed represented the reverse transfer of Fc^+ produced from a heterogeneous ET reaction at the generator into the collector. This procedure is useful for studying the IT of Fc^+ coupling with ET across the L/L interface at the generator, which can be expressed as follows:

$$Fc^+ (DCE) \rightarrow Fc^+ (W) \quad \text{(Coupling IT at generator)}$$

For an ideal simple heterogeneous ET reaction without a coupling IT process, the generator current at any E_g can be calculated as

$$i_g = i_c/\eta_{max}^{ideal} \quad (1)$$

Here, η_{max}^{ideal} is assumed to be 35%, which was evaluated from the experiments of FIT. This assumption is approximate but reasonable in terms of some similarities between a simple heterogeneous ET process and a FIT reaction at a L/L interface.[12] Therefore, the coupling IT of Fc^+ at a generator can be estimated from i_c versus E_g dependence according to the following equation:

$$i_{IT}^{coupling} = i_c/(\eta_{max}^{ideal} - \eta_{max}^{coupling}) \quad (2)$$

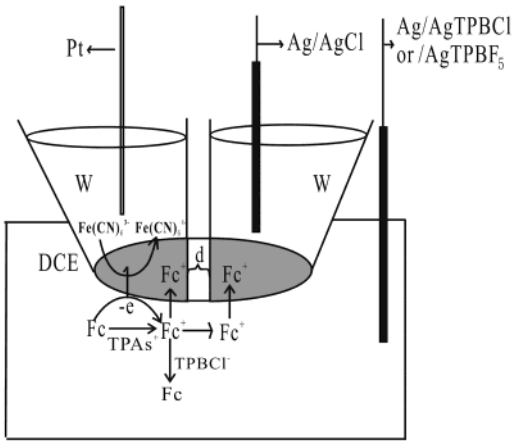

Figure 5. Schematic representation of ET, IT, ET−IT processes occurring at the double-micro-L/L interfaces and the side reactions in the organic phase.

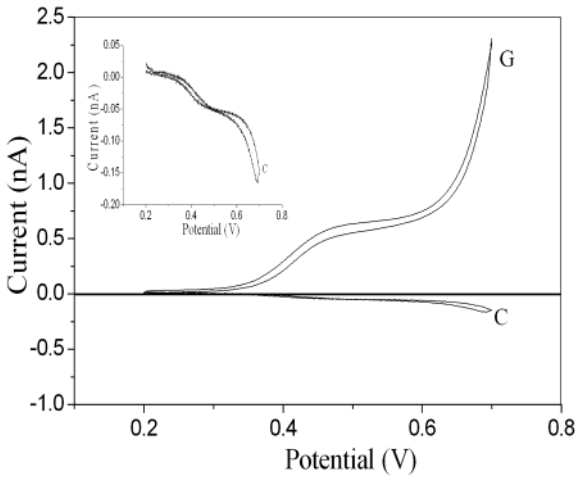

Figure 6. G/C voltammograms of ET obtained employing TBAsTPBF$_5$ as the organic supporting electrolyte. For other parameters, see Figure 3.

where $\eta_{max}^{coupling}$ is equal to 6% as discussed above. As shown in Figure 4B, a well-defined generation voltammogram (curve 2) representing this IT coupling process at the generator was obtained, which indicates that the IT process coupling with ET across the L/L interface at the generator is indeed possible. The ET, IT, ET−IT coupling processes occurring at the double-micro-L/L interface, and the side reactions with the organic supporting electrolyte in the organic phase can be illustrated schematically in Figure 5.

Competing Reactions with the Organic Supporting Electrolyte. We changed the organic supporting electrolyte from TBATPBF$_5$ into TPAsTPBF$_5$ and TBATPBCl to further investige the possible effect of organic supporting electrolyte on this ET process. According to Samec et al.,[20b] there is a possibility of the oxidation of ferrocene to ferricenium in the presence of $TPAs^+$ in the organic phase. Figure 6 showed the G/C voltammograms obtained using TPAsTPBF$_5$ as the organic supporting electrolyte at a double-micropipet, whose geometry is similar to that used in Figure 4A. Both steady-state generation and collection voltammograms (curve G and C) were also obtained. Compared with Figure 4A, it was obvious that the i_g was almost unchanged whereas the i_c became larger, which led to larger collection

efficiency. The collection efficiency was caculated to be 10%, which is also much lower than that of FIT due to the ET−IT coupling process ocurring at the generator, as discussed previously, and possible slower kinetically compared with that of Na^+ transfer (~3.5−6 times slower). However, it is larger than the value obtianed using $TBATPBF_5$ as the organic supporting electrolyte. The larger i_c and η should owe to the collection of excessive Fc^+ produced from the oxidation of Fc by $TPAs^+$ in the DCE solution.

Additionally, as reported by Quinn and Kontturi,[20e] the redox potentials of $TPBCl^-$ and $TPBF_5^-$ on Pt in DCE solution are about 1.0 and 2.1 V versus SHE, respectively, whereas the half-wave potential for Fc is 0.65 V; hence, decomposition of the Fc^+ reaction with $TPBF_5^-$ is almost impossible because of the great difference in redox potentials, but reduction of Fc^+ by $TPBCl^-$ is possible. Figure 7A showed the generation and the collection voltammograms obtained employing TBATPBCl as the organic supporting electrolyte. A well-defined steady-state sigmoidal generation voltammogram (curve G) was observed. The collection voltammogram (curve C) was a characterless curve, and the same results were obtained at different potentials (see the inset in Figure 7A) and at another pipet with different geometry (see Figure 7B), which indicate that few reaction products at the generator can be collected at the collector, and the collection efficiency (η) is nearly equal to zero. Therefore, it can be concluded that the product Fc^+ in the organic phase can not only transfer into the aqueous solution in the generator due to an ET−IT coupling process but also react with the anion of the organic supporting electrolyte $TPBCl^-$ as well (see Figure 5).

IT−IT Coupling Processes. As reported by Mirkin et al.,[19] the double-barrel micropipet technique could also be useful to probe the IT−IT coupling processes occurring at a L/L interface, for instance, the simultaneous transfers of K^+ and $TPBCl^-$ across the W/DCE interface. Figure 8 showed the generation (curve G) and the collection (curve C) voltammograms of simple IT of potassium ion and other alkali metal ions across the W/DCE interface employing cell 3. Obviously, it is difficult to analyze the generation voltammograms due to the IT−IT coupling processes between an alkali metal cation and the anion of the organic supporting electrolyte $TPBF_5^-$. However, unlike the generation voltammograms, the quasi-steady-state sigmoidal collection voltammograms of K^+, Rb^+, and Cs^+ could be obtained at a slow scan rate, which was only due to the reversed transfer of these ions from DCE to water. As for the Li^+ and Na^+ cases, it is difficult to observe the corresponding direct transfer waves from their collector voltammograms, which can be solved by increasing their concentration in the aqueous solution in the generator (see the inset in Figure 8). Thus, this technique is useful for evaluation of the ion-transfer coupling processes happening at the positive end of the potential window. On the other hand, some anions have relatively high Gibbs energies of transfer and their direct transfers at the L/L interface always occur at or near the negative end of the potential window, where the cation of an organic supporting electrolyte, such as $BTPPA^+$, simultaneously transfers from the organic to the aqueous phase. As a result, it is difficult to distinguish anions and to separate the contribution to the current from cation transfer in the opposite direction. This can be solved to lower the Gibbs energy of transfer of anion by selecting an

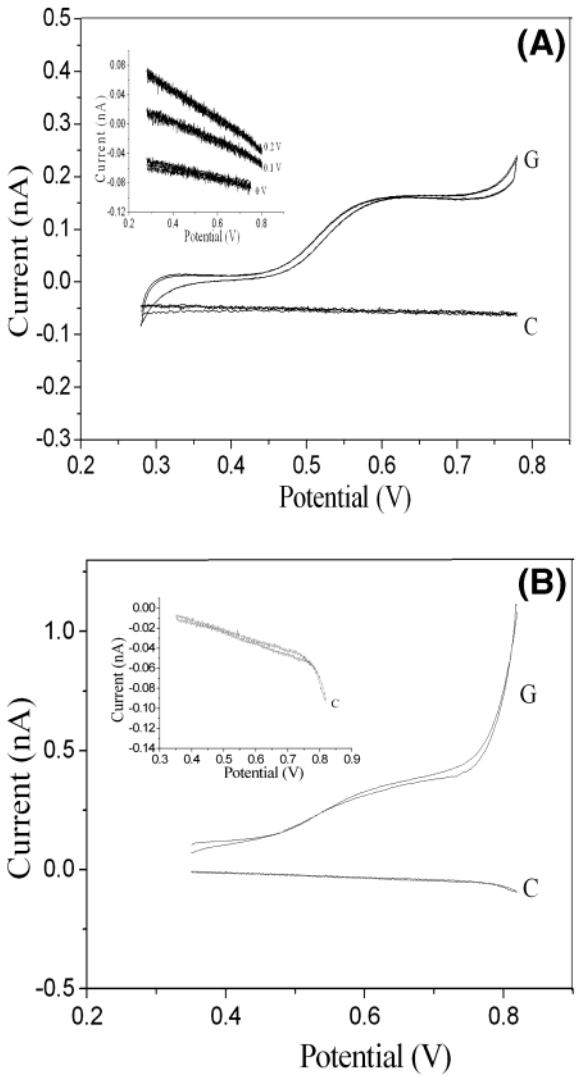

Figure 7. G/C voltammograms of ET obtained employing TBATPBCl as the organic supporting electrolyte at different pipets. (A) $r_g = r_c = 2$ μm and (B) $r_g = r_c = 4$ μm, E_c was 0.1 V vs Ag/AgTPBCl. The inset in (A) was the collection voltammograms obtained at different collecting potentials. Scan rate was 10 mV/s.

ionophore and then shifting the anion-transfer process to within the potential window, namely, "facilitated ion transfer". However, compared with a cation ionophore, so far there have been fewer ionophores found to be suitable to facilitate anion transfer across a L/L interface.[23] Here, we also applied this technique to separate and measure those IT−IT coupling processes appearing at the negative end of the potential window.

Figure 9A showed the G/C voltammograms of the simple ion transfer of NO_3^- at the W/DCE interface using cell 4. An asymmetric generation voltammogram (curve G) was observed due to the asymmetric diffusion field of the double-micro-L/L interface similar with that formed at the tip of a micropipet, but it appeared near the negative end of the potential window resulting in an incomplete peak-shaped wave, which indicates that the

(23) (a) Bakker, E.; Buehlmann, P.; Pretsch, E. *Chem. Rev.* **1997**, *97*, 3083−3132. (b) Buehlmann, P.; Pretsch, E.; Bakker, E. *Chem. Rev.* **1998**, *98*, 1593−1687. (c) Shioya, T.; Nishizawa, S.; Teramae, N. *J. Am. Chem. Soc.* **1998**, *120*, 11534−11535. (d) Qian, Q. S.; Wilson, G.; James, K. B.; Girault, H. H. *Anal. Chem.* **2001**, *73*, 497−503.

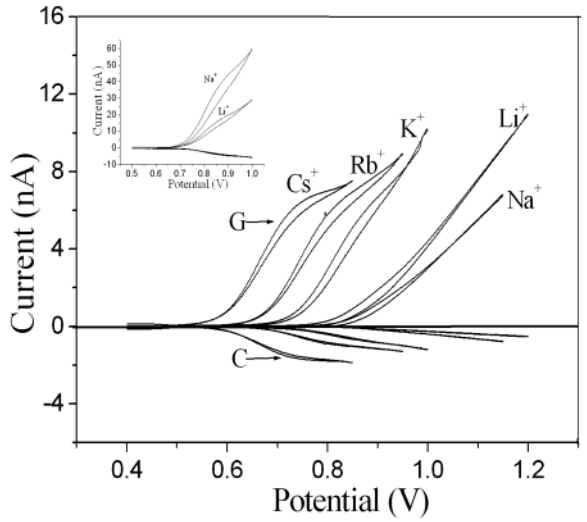

Figure 8. G/C voltammograms of simple cation transfer of Li^+, Na^+, K^+, Rb^+, and Cs^+ across the W/DCE interface using cell 3. The generator consisted of 10 mM LiCl, NaCl, KCl, RbCl, and CsCl, respectivly. Both orifices of the double-barrel micropipet were 6 μm in radius. The inset showed the G/C voltammograms obtained under higher concentration of Li^+ and Na^+ (0.1M) in the generator. E_c was 0.2 V vs Ag/AgTPBF$_5$. Scan rate was 10 mV/s.

transfer of NO_3^- from W to DCE was partly coupled with the transfer of the cation of organic supporting electrolyte $BTPPA^+$ in the opposite direction. When the collector was held on the positive potential ($E_c = 0.4$ V), it was unfavorable for the transfer of cation $BTPPA^+$ from the outer organic solution into the aqueous solution in the collector, so that a well-defined quasi-steady-state sigmoidal collector voltammogram (curve C) could be obtained, which only represents the reversed transfer of NO_3^- without an ion-transfer coupling process to the collector. In addition, the collection current was also governed by the collecting potential (see the inset of Figure 9A).

For other anions with Gibbs energies of transfer higher than those for NO_3^-, such as NO_2^- and Cl^-, their direct transfer waves should appear at more negative potential, so that it is more difficult to distinguish their direct transfer from the coupling ion transfer in the opposite direction. As shown in Figure 9B, the generation voltammogram of the transfer of NO_2^- from W to DCE (curve G) appeared completely at the negative end of the potential window, which indicated that the NO_2^- transfer at the generator was coupled strongly with the transfer of $BTPPA^+$ in the opposite direction. If the collection potential was held positively ($E_c = 0.2$ V), the collection voltammogram (curve C) due to the direct reversed transfer of NO_2^- from the organic phase into the collector could also be observed, but the collection voltammogram was not as well-defined as that of NO_3^-. A more well-defined quasi-steady-state sigmoidal collector voltmmogram can be obtained in a different way (see the inset in Figure 9B), namely, by holding the generator potential at -0.2 V, while scanning the collector from -0.2 to $+0.2$ V.

Furthermore, it was found that transfers of two anions across the same interface could be simultaneously collected. Figure 10A showed the generation and the collection voltammograms of the transfer of two anions ClO_4^- and Cl^- across the W/DCE interface using cell 3. In the middle of the potential window, a well-defined asymmetric generator voltammogram (curve G) and a well-defined

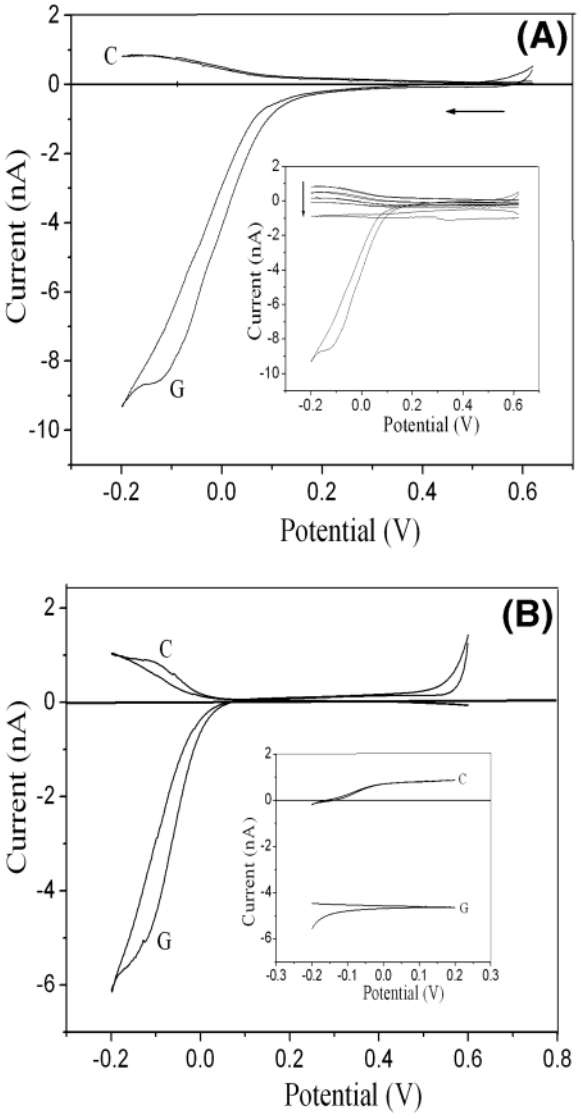

Figure 9. G/C voltammograms of simple anion transfer across the W/DCE interface. (A) NO_3^- obtained using cell 4 where $x = 10$ mM, Y = $LiNO_3$ at a pipet ($r_g = 8$ μm; $r_c = 7$ μm), E_c was 0.4 V vs Ag/AgTPB. The inset was that obtained at different collecting potentials (E_c was 0.4, 0.2, 0, -0.1, and -0.2 V from top to bottom). (B) NO_2^- obtained using cell 4 where $x = 10$ mM, Y = $NaNO_2$ at a pipet ($r_g = 4$ μm; $r_c = 3$ μm), E_c was 0.2 V vs Ag/AgTPB. The inset was the G/C voltammograms obtained when E_g was held on -0.2 V and E_c was swept within -0.2–0.2 V vs AgTPB. Scan rate was 10 mV/s.

quasi-steady-state collection voltammogram (curve C) for the transfer of ClO_4^- across the W/DCE interface were obtained due to the relatively low Gibbs energy of transfer of ClO_4^-. Moreover, as shown in Figure 10A, it is also difficult from the generation voltammogram to observe the direct transfer of anion Cl^- from W to DCE because of the strong coupling transfer of $BTPPA^+$ in the opposite direction. However, a quasi-steady-state sigmoidal collection voltmmogram for the reversed transfer of chloride could be observed at the negative end of the potential window, which was obtained more clearly when the aqueous solution in the generator only contained the electrolyte LiCl (see the inset in Figure 10A).

The IT–IT coupling transfer processes discussed above focused mainly on the coupling ion transfer in the opposite

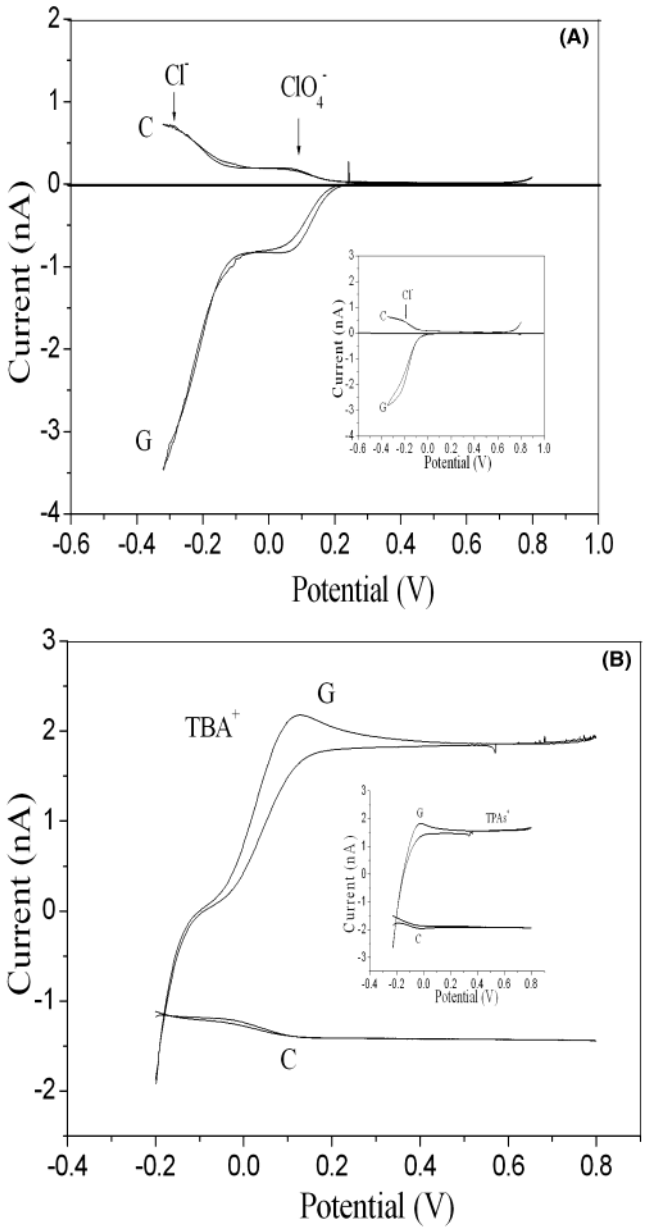

Figure 10. (A) Simutaneous collection of two anions ClO_4^- and Cl^- at the W/DCE interface employing cell 3. Where $x = 2$ mM, Y = $NaClO_4$, E_c was 0.4 V vs $AgTPBF_5$. The inset was the G/C voltammograms of Cl^- obtained employing cell 3 without $NaClO_4$ in the generator, E_c was 0.5 V vs Ag/$AgTPBF_5$. (B) The G/C voltammograms of TBA^+ and $TPAs^+$ (the inset) obtained employing cell 3, where the generator only contained 10 mM TBACl or TPAsCl, repectively. E_c was −0.2 V vs Ag/$AgTPBF_5$. Scan rate was 10 mV/s. Both orifices of the double-barrel micropipet used in the experiments were 4 μm in radius.

direction. In fact, IT−IT coupling transfer processes can occur in the same direction. Figure 10B showed the generation and collection voltammograms for relatively hydrophobic cation TBA^+ transfer across the W/DCE interface. From the generation voltammogram (curve G), it is obvious that the cation TBA^+ transfer from W to DCE was partly coupled with the simultaneous transfer of chloride in the same direction. When the collector was held at negative potential ($E_c = -0.2$ V), the transfer of chloride from DCE to W was unfavorable, so the direct reversed transfer of cation TBA^+ without coupling transfer of chloride could be observed (curve C). As for more hydrophobic cation $TPAs^+$, the collection voltammogram representing its direct transfer from DCE to W could be also obtained by employing the same method (see the inset in Figure 10B).

Table 1. Thermodynamic Data from the Experiments and from Literature for Ion Transfer Across the Water/1,2-Dichloroethane Interface

ion	$\Delta_o^w\phi^{o'}$ (V)	$E_{1/2}^c$ (V)	$\Delta_o^w\phi_{exp}^{o'}$ (V)	$\Delta G^{o,w\to o}$ (kJ/mol)	$\Delta G^{o',w\to o}$ (kJ/mol)
Li^+	0.598[a]	0.87	0.56	57[a]	54
Na+	0.584[a]	0.87	0.56	57[a]	54
K^+	0.526[a]	0.81	0.50	50[a]	48
Rb^+	0.445[b]	0.75	0.44	42[b]	42
Cs^+	0.381[b]	0.66	0.35	35[b]	34
$TPAs^+$	−0.365[c]	−0.097	−0.407	−39.7[d]	−39.3
TBA^+	−0.225 [c]	0.034	−0.276	−29.4[d]	−26.6
Cl^-	−0.526[a]	−0.21	−0.52	51[a]	50
NO_3^-		−0.021	−0.28	30.3[e]	27
NO_2^-		−0.075	−0.334		32
COO^-		−0.16	−0.44		42.5
TEA^+	0.019[c]	0.278		1.8[c]	
ClO_4^-	−0.170[c]	0.14		16.4[c]	

[a] Data were from ref 24. [b] Data were from ref 25. [c] Data were from ref 26. [d] Data were from ref 27. [e] Data were from ref 28. $E_{1/2}^c$ is the half-wave potential of ionic collection voltammogram. For Li^+ and Na^+, the influence of higher-concentrated Cl^- in the generator to $E_{1/2}^c$ was subtracted from the $\Delta_o^w\phi_{exp}^{o'}$.

According to the half-wave potential of these quasi-steady-state collection voltmmograms obtained above and the formal Galvani potential difference of reference ions (ClO_4^- for cell 3, TEA^+ for cell 4), the formal Galvani potential difference and the formal Gibbs transfer energies for the direct transfer of these ions from water to DCE can be evaluated based on the relationships in following the equations:

$$E_A^{1/2} - E_R^{1/2} = \Delta_o^w\phi_A^{o'} - \Delta_o^w\phi_R^{o'} \quad (3)$$

$$\Delta G^{o',w\to o} = \pm nF\Delta_o^w\phi_A^{o'} \quad (4)$$

where A is the transferred ion, R is the reference ion, F is the Faraday constant, and negative and positive signs refer to the respective anion and cation. For other very strong hydrophilic anions, such as phosphate, sulfate, carbonate, and acetate, we found that it is difficult to observe their corresponding direct transfer wave by this method (except acetate). There are two possible reasons: one is that their Gibbs energies of transfer are much higher than that of $BTPPA^+$ (its transfer potential limits the negative end of the potential window); and another is due to the formation of an ion pair between the di- or trivalent anion in the aqueous solution and the cation of the organic electrolyte at the interface. The resulting experimental data are listed in the Table 1 and compared with the values reported previously.[24−28] The mutual difference between them indicates this technique is an effective and approximate method to separate and measure

(24) Sabela, A.; Mareček, V.; Samec, Z.; Fuoco, Z. *Electrochim. Acta* **1992**, *37*, 231−235.
(25) Samec, Z.; Mareček, V.; Colombini, M. P. *J. Electroanal. Chem.* **1988**, *257*, 147−154.

the direct transfer of those strongly hydrophilic or hydrophobic ions from the coupling processes occurring at the W/DCE interface.

CONCLUSIONS

A double-barrel micropipet technique employed as a generation/collection device has been demonstrated to be a very useful qualitative and quantitative tool to study ET and the charge-transfer coupling processes including ET−IT and IT−IT occurring at the W/DCE interface. The results indicate that the ET reaction between $Fe(CN)_6^{3-}$ in the aqueous phase and ferrocene in DCE can be complicated by various side reactions, especially the ET−IT coupling process and the competing reactions with the organic supporting electrolyte. According to the generation and collection currents as well as collection efficiency, the charge-transfer coupling process between ET and IT across the W/DCE interface was distinguished and measured. Moroever, the direct transfers from W to DCE of some strongly hydrophilic or hydrophobic ions, such as NO_3^-, NO_2^-, Cl^-, COO^-, TBA^+, $TPAs^+$, Cs^+, Rb^+, K^+, Na^+, and Li^+, were observed, and their formal transfer potential and formal Gibbs energies of transfer across the W/DCE interface were evaluated by using this technique to separate the IT−IT coupling processes occurring in the opposite or same direction. Experiments simulating the mass transport processes involving in such G/C technique are being conducted in our laboratory.

(26) Wandlowski, T.; Mareček, V.; Samec, Z. *Electrochim. Acta* **1990**, *35*, 1173−1175.

(27) Shao, Y.; Stewart, A. A.; Girault, H. H. *J. Chem. Soc., Faraday Trans.* **1991**, *87*, 2593−2597.

(28) Hundhammer, B.; Solomon, T. *J. Electroanal. Chem.* **1983**, *157*, 19−26.

ACKNOWLEDGMENT

The authors acknowledge the National Natural Science Foundation of China (Grants 29835111, 20173058, and 20235010**)**, and the special 985 project of Peking University for financial support of this work.

Received for review June 22, 2003. Accepted September 25, 2003.

AC034674E